Civil Engineering and Applied Solutions

Research Article

journal homepage: ceas.journals.umz.ac.ir

CEAS Civil Engineering and Applied Solutions

Reliability Assessment of Steel Structure Subjected to Blast Loading Using Monte Carlo Sampling

Zeinab Meghdadi [a], Mohammad Shabanlou [a*]

[a] *Department of Civil Engineering, Sharif University of Technology, Tehran, Iran*

A R T I C L E I N F O

Article history:

Received 29 April 2026

Revised 04 June 2026

Accepted 07 August 2026

Available online 01 April 2027

Keywords:

Steel plate shear wall

Probabilistic modeling

Monte Carlo

Blast loading

A B S T R A C T

In recent years, the occurrence of accidental or deliberate explosions has prompted engineers to consider the effect of explosive blast load on the overall performance of structures. Normally, residential structures are designed to resist conventional design loads such as gravitational, earthquakes, wind, and snow. In this research, a steel structure with a lateral load-bearing system of steel plate shear wall has been subjected to explosive blast load. Uncertainty in structural components as well as blast loading can lead to an incorrect and erroneous estimate of the structural response to blast. This study investigates the reliability of a steel structure under blast load, taking into account the uncertainty in the distance between the blast charge and the structure, the weight of the blast charge, the wall plate thickness, the yield stress of the wall plate, the yield stress of the beam and column of the structure. The probability of failure is then obtained by modeling the structure in OpenSees software and generating 1700 samples using Monte Carlo sampling method. Results indicated that the probability of failure of the mentioned system under the blast load is 55% and the most effective parameter is web plate thickness.

How to cite this article: Meghdadi, Z., Shabanlou, M. Reliability Assessment of Steel Structure Subjected to Blast Loading Using Monte Carlo Sampling. Civil Engineering and Applied Solutions. 2027; 3(2): 131–143. doi:10.22080/ceas.2026.31632.1096.

1. Introduction

Conventional steel structures are often designed considering regular loads such as earthquake and wind. However, structures are prone to internal or external explosions during their lifetime, which brings catastrophic damage to buildings and results in causalities. Therefore, the blast response of structures and identifying their residual operational performance is of great importance. Additionally, an important characteristic for blast-subjected structures is the difference in the material properties. For instance, as the strain rate is high in blast loading, the yield stress of steel increases significantly while the elastic modulus remains the same.

Recently, the use of steel plate shear wall (SPSW) as a lateral load-bearing system for steel structures has increased. The main components of a SPSW system are beams and columns, also known as boundary members and steel web plate. High strength and stiffness characteristics, stable hysteresis loops, considerable energy dissipation capacity, high ductility, and redundancy are important advantages of SPSW systems [1-3].

Preserving human lives and the protection of equipment and assets are two important aspects of engineering. Therefore, structures are designed for gravitational and lateral loads based on the current design codes. Financial concerns, as well as the low probability of high-risk loads such as impact or explosion, usually cause these loads to be excluded from the design process. Normally, only military structures or special structures are designed and controlled for the mentioned loads. However, with the increase in the possibility of terrorist attacks and blast incidents, it seems necessary to have a good insight on the performance of normal residential structures against explosions. Many studies have focused on reliability analysis of structures when exposed to explosive blast loading. Stewart et al. performed a reliability analysis to assess the risks of damage caused by blast loading to

* Corresponding author.
E-mail addresses: mohammad.shabanlou@sharif.edu (M. Shabanlou).

https://doi.org/10.22080/ceas.2026.31632.1096
ISSN: 3092-7749/© 2027 The Author(s). Published by University of Mazandaran.

infrastructure and proposed a probabilistic risk assessment procedure [4]. Al-Hababheh and Stewart [5] conducted a structural reliability analysis of unreinforced brick masonry walls subjected to explosive loading. Using Monte Carlo sampling method, the failure probability shows that the wall has a very high reliability when subjected to explosive blast loading. In a study conducted by Shi and Stewart, blast reliability curves for RC columns under blast loading for different threat scenarios were generated using Monte Carlo sampling method [6]. The results showed that by considering spatial variability of concrete compressive strength and concrete cover, the probability of failure increases. Stewart and Netherton compared field test results with reliability-based computer analysis and proposed design load factors for different reliability levels. For instance, the load factor for a 0.99 reliability level will be as high as 1.30 [7, 8]. Stochino conducted a parametric and reliability study on the response of reinforced concrete beams under explosive loads [9]. Results showed that slenderness and peak load value were the most effective parameters affecting the beam response. Thomas et al. investigated the effect of vehicle collision and explosive loads on the reliability of bridge columns using a 1st-order 2nd-moment reliability study [10, 11]. The most affective parameter affecting the reliability of structures subjected to explosive loading was demonstrated to be the diameter of the column and the standoff distance of the blast.

The aim of the current study is to further focus on the reliability of steel structures with an SPSW system under blast loading. The parameters that are investigated here are the scaled distance, the infill plate thickness, the plate yield stress, and the yield stress of the structure's beam and column.

2. Steel plate shear wall system

The steel plate shear wall (SPSW) works as a lateral bearing system, comprising an infill web plate in a rigid frame, with the frame members serving as the boundary members of these plates. In a frame with multiple stories, the SPSW system can be likened to cantilever girders, where the columns act as flanges, floor beams like stiffeners, and at the end, steel web plates as the girders web [12-14]. However, as the stiffness of the flanges in plate girders is insufficient, SPSWs are fundamentally different from plate girders in terms of structural performance. In other words, as the stiffness of columns is very high in SPSW, the tension field expands in the whole area of the plate, but this phenomenon is not possible in a conventional plate girder [15].

The SPSW system demonstrates a stable hysteresis loop, rendering it a dependable option as a lateral structural system [16]. The shear actions are resisted by a field of tension created in the SPSW. The web plate does not provide remarkable strength in the linear elastic region; however, it is known for its high post-buckling strength [17-20]. According to the concept of capacity design, the tension field which is formed in the steel plate, imposes forces on the boundary elements. So columns and beam shall be designed in such a way to resist this force [21-23]. Also, Seismic assessment of the SPSWs reveals sufficient ductility, stiffness, and energy absorption [24-26].

3. Structural design

The structural design is performed in accordance with AISC 360 [27] and AISC 341 [28], while the seismic and gravity loads are determined based on ASCE 7-16 [29]. The considered building represents a conventional residential steel structure located in a region with high seismicity. Therefore, the structural configuration and member sizes are selected to satisfy the requirements of standard seismic design practice rather than special blast-resistant design provisions.

The perimeter beams of the SPSW system are connected to the columns using rigid connections, while the remaining beams (gravity beams) are modeled with hinged connections [30]. The structure is designed to resist the demands resulting from gravitational and seismic loading. According to AISC 341 [28], the aspect ratio of steel plate shear walls should be between 0.8 and 2.5, and this requirement is satisfied in the present model.

The prototype structure is a three-story building with a story height of 3.3 m and a bay span of 5 m. Four SPSW bays are located on the perimeter of the building, and the structure was initially analyzed and designed using a three-dimensional model. After completing the design process and finalizing the structural sections, including columns, beams, and steel plate thickness, one representative perimeter frame was extracted and modeled as a two-dimensional frame in OpenSees [31] for the nonlinear dynamic analyses. The schematic view of the structural model is shown in Fig. 1.

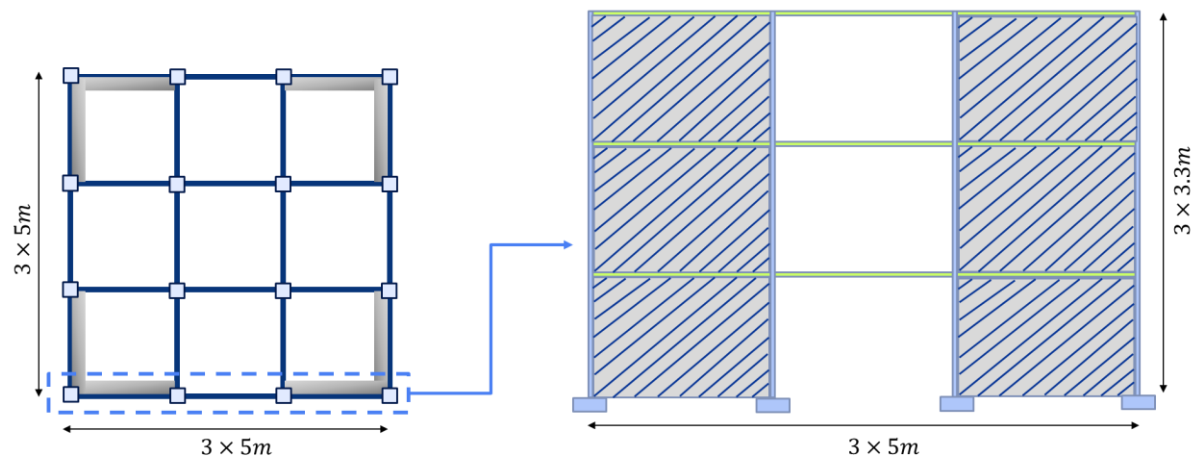

Fig. 1. Schematic view of the studied structure.

In the considered building, two SPSW systems are present in each principal direction. Therefore, the blast load applied to the structure is assumed to be equally shared between the two frames, and half of the calculated blast pressure is applied to the analyzed frame.

In the selected frame, the columns consist of box sections (BOX 200×20). The boundary beams at the first and second stories are plate girders with web dimensions of 350×8 mm and flange dimensions of 200×20 mm. The boundary beams at the third story are plate girders with web dimensions of 400×10 mm and flange dimensions of 300×25 mm.

4. OpenSees modelling and verification

4.1. Numerical model

The structure was modeled and analyzed using the nonlinear analysis software OpenSees [31]. The strip model introduced by Thorburn et al. [32] was utilized. Also, the newest material model developed by Jalali et al. [33-35]. The area of cross-section of each truss element is correlated with the steel plate thickness by Eq. 1 [30].The variables α, t_w, h, L, and n represent the web plate inclination angle, thickness of the wall, the height and length of the wall, and the number of strip truss elements, respectively.

$$A_s = \frac{[L\cos(\alpha) + h\sin(\alpha)]}{n} t_w \quad (1)$$

To capture the behavior of beams and columns, a plasticity distributed model with nonlinear elements was implemented. The modeling approach assumes that entering the nonlinear region is possible for every point of the elements, allowing for use of materials with nonlinear behavior along the length of the element for the analyze.

To simulate the steel plate shear wall, 10 truss elements were employed in each direction, meeting the minimum number of recommendations outlined in AISC 341-16 [28]. Consequently, the wall was composed of 20 truss strip elements in each infill panel.

In OpenSees, the Steel02 material, a strain-hardening isotropic steel with yield stress F_y = 235 MPa, modulus of elasticity E_s = 206 GPa, and a strain-hardening ratio of 0.01, is utilized to model beams and columns. Additionally, the SPSW02 material proposed by Jalali and Banazadeh [33, 34] is employed to model the strips equivalent to the infill plate. Also, a material with the same properties is used for the columns and beams. The cyclic behavior of this material is illustrated in Fig. 2, with $\sigma_{max,1}$ representing the ultimate stress of the main loading cycle.

The use of equivalent strip elements for the infill plate allows the numerical model to represent the post-buckling behavior of the SPSW system. After buckling, the steel plate contributes to the lateral resistance mainly through tension-field action, which is captured by the nonlinear response of the SPSW02 strip elements. Therefore, the global nonlinear behavior of the SPSW system is simulated through the interaction between the boundary beams, boundary columns, and the yielded plate strips. In the reliability analysis, the yield stress of the steel infill plate and the yield stress of the boundary beams and columns were considered as uncertain parameters. The elastic modulus was assumed to remain unchanged, which is consistent with the adopted treatment of high-strain-rate effects, where the steel yield stress is modified while the elastic stiffness is maintained.

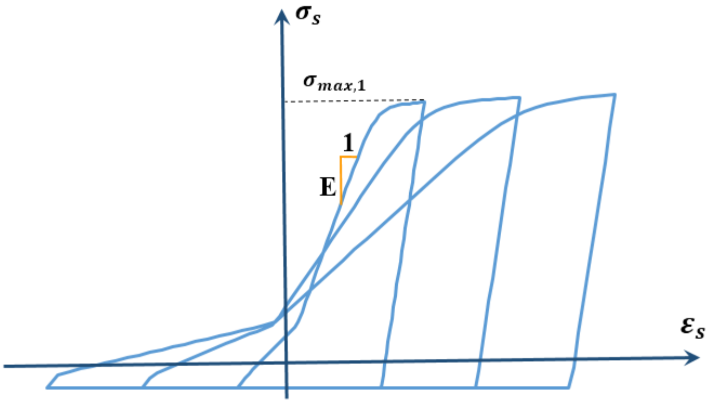

Fig. 2. Cyclic performance of SPSW02 model in OpenSees.

In the nonlinear dynamic analyses, viscous damping was modeled using Rayleigh damping implemented in OpenSees. In this approach, the damping matrix is constructed as a combination of mass-proportional and stiffness-proportional components. In the present model, the damping formulation includes a mass-proportional term and a stiffness-proportional term based on the last committed stiffness matrix of the structure.

The damping coefficients were determined to achieve a target damping ratio of 5%, which is commonly adopted for steel building structures in the literature. The coefficients were calculated using the first and fifth natural vibration modes of the structure obtained from eigenvalue analysis. The circular frequencies of these modes were determined from the corresponding eigenvalues, and the Rayleigh damping parameters were then calculated based on the selected modal frequencies and the target damping ratio.

This damping formulation was applied consistently to all nodes and elements of the numerical model, and the same damping parameters were used in all nonlinear time-history analyses performed for the blast loading simulations.

4.2. Verification

The numerical simulation in OpenSees was verified with an experimental specimen from a test performed by the study of Sabouri-Ghomi and Sajjadi [36]. The specimen was a single-story SPSW, with an aspect ratio of 1.46. The wall infill plate was modeled using the strip model corresponding to 20 trusses with material of SPSW02 as in studies by Jalali and Banazadeh [33, 34]. In addition, the boundary members were modeled using steel02 material with non-linear elements of steel. The results obtained from the cyclic experiment showed good agreement with numerical results. It is important to note that there are no experiments on the behavior of SPSW under blast loading to be used as a reference for verification purposes. Based on FEMA 427 [37], it is possible to model the explosive blast load as a quasi-static load (pressure load). So, to get the most similar reliable results, verification was carried out by implementing a cyclic loading model that is comparable to blast numerical modeling implemented herein. The comparison of test specimen and numerical results can be observed in Fig. 3.

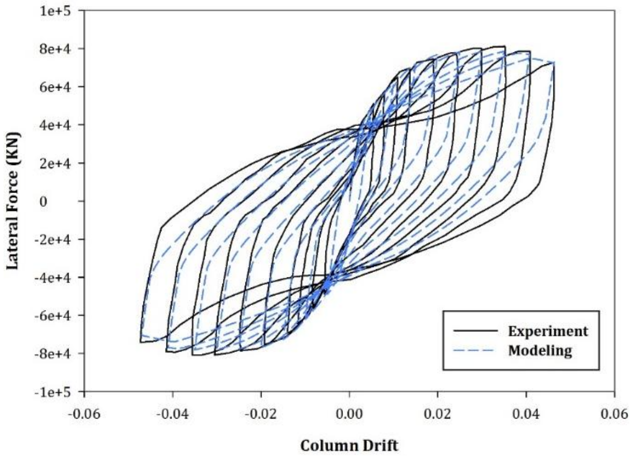

Fig. 3. Verification of experimental specimen with numerical model.

5. Blast loading

Blast loading significantly exceeds the structural design forces and is applied over a brief period of time. The structural performance under blast and ballistic loading is highly intricate, influenced by factors such as high strain rate, elevated temperature, and propagation of blast waves within the structure. This study examines the behavior of a steel structure with an SPSW system under external blast loading, which occurs when the explosive charges are situated outside the structure.

To accurately simulate these conditions, the blast loading was determined using empirical relationships based on the charge weight and standoff distance, consistent with the procedures described in UFC 3-340-02. The blast event was characterized by estimating the incident overpressure and the peak reflected pressure. For the 2D OpenSees model, the complex time-varying blast wave was simplified into an equivalent triangular pressure-time pulse, which is a standard engineering approximation for structural response analysis.

To account for the 3D nature of the building in a 2D framework, the total blast pressure acting on the building front was distributed across the primary structural frames. Since the structure contains two identical SPSW systems in each principal direction, the total blast load was halved and applied to the 2D analytical frame as a uniformly distributed time-varying load acting on the front-facing columns and beams. The spatial distribution of this pressure was calculated based on the tributary area of the structural members. In this analysis, only the positive phase of the blast pressure was considered; negative phase effects and pressures on the back face of the structure were neglected to maintain a conservative estimate of the structural response.

5.1. Dynamic properties of materials

Blast loading results in very high strain rates ranging from 10^2 to 10^4 s^{-1}, whereas the rate of strain in static condition falls between 10^{-6} to 10^{-5} s^{-1} [38]. These high strain rates change the dynamic mechanical properties of the structure, leading to different types of failure in various members of the structure. The impact of large values of strain rates on the properties of steel has been the subject of numerous studies [39].

It has been observed that high strain rates significantly influence material properties, resulting in changes in the flow of the plastic stresses and material ductility during impulsive loadings. With increasing strain rates, both the yield and ultimate tensile stress also rise significantly [40]. Yield stress (f_{dy}) and also ultimate stress of design in dynamic state (f_{du}), can be obtained by modifying the pure mentioned stresses through strength and dynamic increasing parameters, respectively (Eqs. 2 and 3) [41].

$$f_{dy} = (SIF) \times (DIF) \times f_y \tag{2}$$

$$f_{du} = (SIF) \times (DIF) \times f_u \tag{3}$$

SIF is a strength rise parameter as defined in Table 1. Additionally, DIF is the dynamic increasing parameter and is provided for steel members, as tabulated in Table 2.

Table 1. Resistance coefficients for various materials.

Material	SIF
S500 rebar	1.15
Rolled steel ST37 and ST52	1.15
Plate girders and other plate-made sections	1.15

Table 2. Dynamic increasing parameter (DIF) for common steel materials.

	Yield stress		Ultimate stress
Loading type material	Bending-shear $\frac{f_{dy,y}}{f_y}$	Compression-tension $\frac{f_{dy,y}}{f_y}$	All $\frac{f_{du,u}}{f_u}$
ST37	1.3	1.2	1.1
ST52	1.2	1.15	1.05

The dynamic increasing parameter is utilized to adjust static strength values in order to account for the impact of high strain rates on material strength. This factor is influenced by the type of stress, such as bending or direct shear. Flexural stresses develop rapidly, while shear strain rates are relatively low, resulting in delayed maximum shears. For axial members subjected to compressive or tensile forces, the strain rate is lower compared to flexural members. Experimental evidence indicates that the modulus of elasticity in dynamic condition remains unchanged in steel materials. Therefore, the yielding strength increasing coefficient for beams was 1.495, and for columns and the steel plate shear wall, this value has been considered equal to 1.38.

5.2. Blast load on front face

The front face is exposed to a two-line pressure pattern, resulting in an equivalent triangular pressure as shown in Fig 4. The maximum over-pressure on the front face, also referred to as the front wave of the explosive blast, is equal to the pressure of reflection (p_r). This pressure reaches the decay state (p_s) at the leveling time (t_c) [41-43].

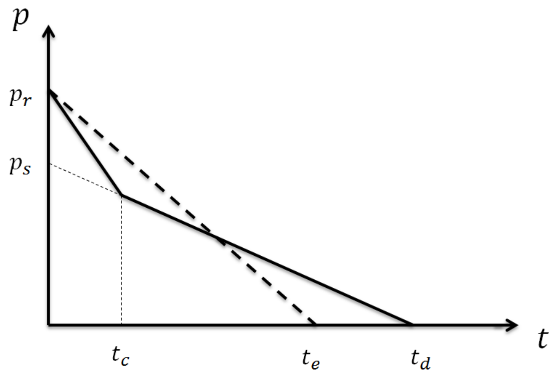

Fig. 4. Blast load on front face.

The leveling time (t_c) is defined by S, G, R, and C_r parameters (Eq. 3). S and G are levelling distances, defined by Eqs. 4 and 5, and R is the ratio of S/G. In addition, C_r is the velocity of sound, which can be obtained from the graph of Fig. 5.

$$t_c = \frac{4S}{(1+R)C_r} \tag{4}$$

$$S = min\left\{B\,;\,\frac{H}{2}\right\} \tag{5}$$

$$G = max\left\{B\,;\,\frac{H}{2}\right\} \tag{6}$$

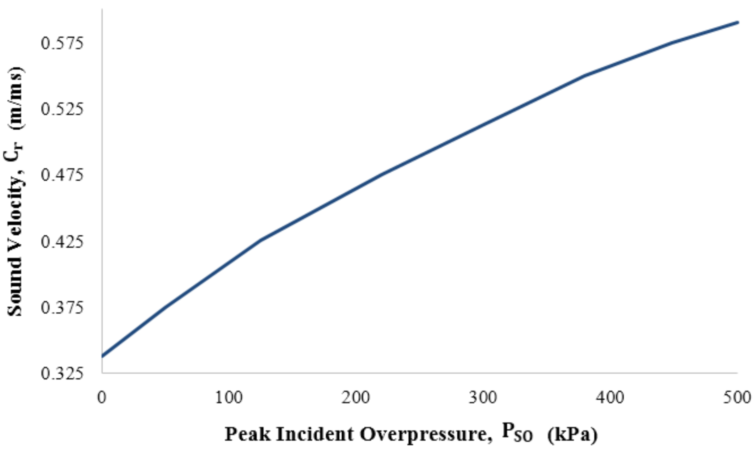

Fig. 5. C_r values as a function of peak incident over-pressure.

Furthermore, the parameters $P_{SO,}$ which is the peak over-pressure of the explosion, and t_e are obtained based on Eqs. 7 to 9.

$$P_S = P_{SO} + C_d q_s \tag{7}$$

$$q_s = \frac{5P_{SO}^2}{2(P_{SO}+7P_0)} \tag{8}$$

$$t_e = (t_d - t_c)\frac{P_S}{P_R} + t_c \tag{9}$$

5.3. Blast load on side face and roof

As there is no reflection wave, the blast load subjecting to the side faces are less than the blast loads on the front face. The triangular blast load with the maximum value of P_a is presented in Fig. 6. P_a is determined using C_e, q_s, C_d, and λ_{rw} parameters by Eq. 10. $C_{e,}$ which is the blast reduction coefficient, is obtained using Fig. 7 [41, 43]. q_s is the maximum dynamic pressure, and C_d is the drag coefficient calculated using Table 3. Also, λ_{rw} is the blast wave length calculated using Eq. 9.

$$\lambda_{rw} = U_s \times t_d \tag{10}$$

$$U_s = 340\sqrt{1 + 0.83P_{SO}} \tag{11}$$

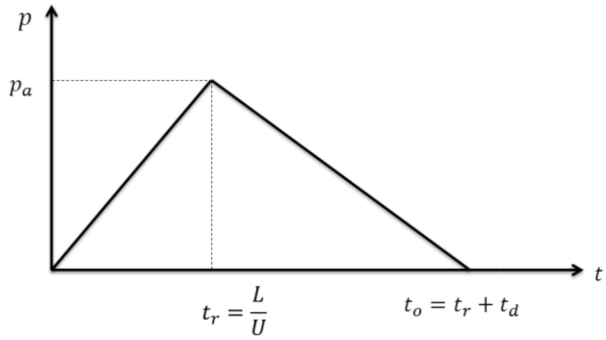

Fig. 6. Blast load on side face and roof.

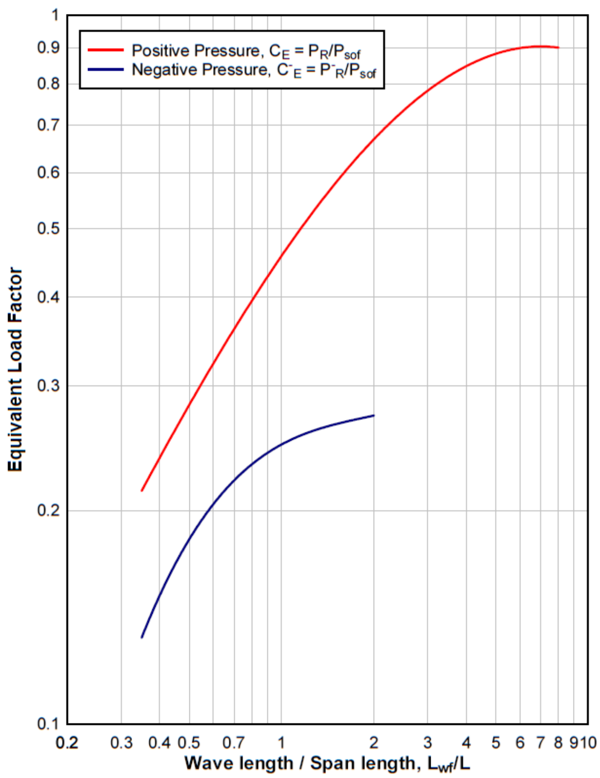

Fig. 7. Blast reduction coefficient.

Table 3. Drag coefficient (C_d).

Maximum dynamic 0ressure (q_s) (kg/cm²)	Drag coefficient (C_d)
0-1.75	-0.4
1.75-3.5	-0.3
3.5-9	-0.2

5.4. Blast load on back face

The equation used for calculation of P_a for the back face is the same as for the side faces. However, for calculation of the C_e value, the height (H) and the length of the building (L) are summed up as shown in Fig. 8. Blast loads on the front face and back face act in the opposite direction, resulting in a reduction in the final value of blast load. Therefore, the blast load on the back face is neglected conservatively [41].

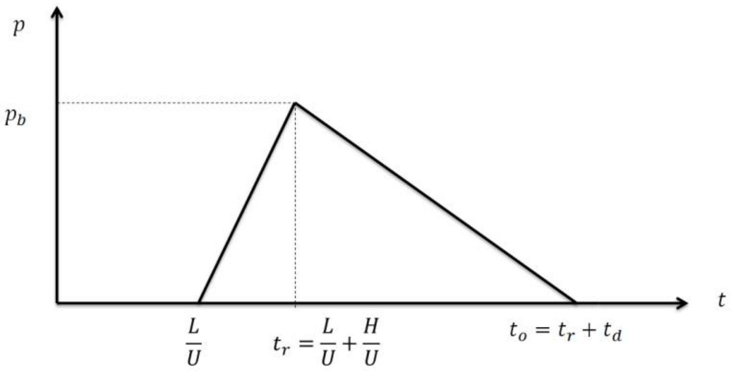

Fig. 8. Blast load on back face.

5.5. Applying blast load

The method of explosive charge and its standoff distance was used to determine the blast type and, therefore, the calculation of incident overpressure, peak reflected pressure, and blast duration. According to the US homeland security document [44], explosive charges and their improvised explosive devices can be categorized as depicted in Fig. 9. In this study, a charge weight (W) equal to 1814 kg was selected and situated at a standoff distance (R) equal to 20 m from the structure, as illustrated in Fig. 10.

Improvised Explosive Device	Explosive Capacity
	227 kg
	454 kg
	1814 kg
	4536 kg
	27215 kg

Fig. 9. Types of explosive charges.

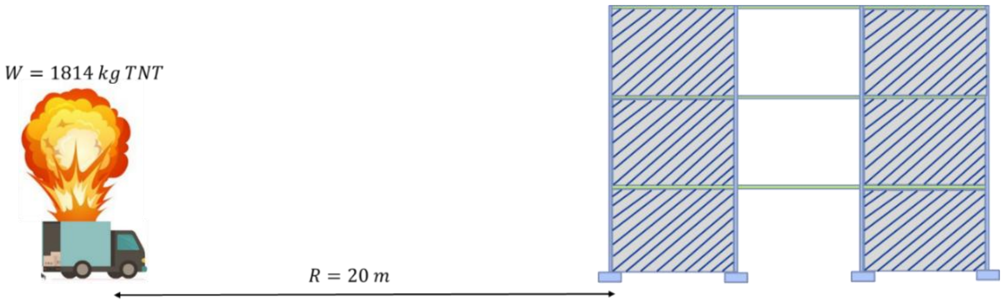

Fig. 10. Standoff distance.

The blast parameters, including the incident overpressure (P_{SO}) and blast duration (t_d), were determined using empirical relationships based on the scaled distance $Z = R/W^{1/3}$. Following the methodology of Moghaddam et al. [45], these parameters were estimated utilizing the empirical approaches proposed by Brode [46] and Newmark and Hansen [47], which are standard for surface blast analysis. These parameters can be calculated using Eqs. 12 to 14.

$$Z = \frac{R}{W^{\frac{1}{3}}} \tag{12}$$

$$t_d = W^{\frac{1}{3}} \frac{980\left[1+\left(\frac{Z}{0.54}\right)^{10}\right]}{\left(\left[1+\left(\frac{Z}{0.02}\right)^{3}\right]\times\left[1+\left(\frac{Z}{0.74}\right)^{6}\right]\times\left[1+\left(\frac{Z}{6.9}\right)^{2}\right]\right)} \tag{13}$$

$$P_{SO} = P_0 \frac{808\left[1+\left(\frac{Z}{4.5}\right)^{2}\right]}{\left(\left[1+\left(\frac{Z}{0.048}\right)^{2}\right]\times\left[1+\left(\frac{Z}{0.32}\right)^{2}\right]\times\left[1+\left(\frac{Z}{1.35}\right)^{2}\right]\right)} \tag{14}$$

6. Structural reliability analysis

As the failure modes of the structural systems are not independent statistically, nor are they entirely dependent, the analysis of reliability is intricate. The demand and capacity are not statistically independent, and the structural performance will be determined from a non-linear finite element analysis.

Optimization is the main pillar for the first-order reliability method (FORM); therefore, this method is susceptible to nonconvergence problems, particularly in dynamic problems. A crucial element for achieving convergence is the requirement for the limit-state function to possess continuous differentiability. Consequently, models containing discontinuities and piecewise functional forms are deemed unfeasible within the First Order Reliability Method (FORM) unless appropriate smoothing techniques are applied [48]. This makes FORM less appealing for engineering purposes in the construction industry. Moreover, in blast loading applications where nonlinear dynamic problems are prevalent, the calculation of the index of reliability using FORM necessitates the linearization of the function of limit-state, potentially resulting in unreliable reliability indices.

Therefore, the damage probability can be derived from a stochastic finite element analysis that will employ event-based Monte Carlo Simulation (MCS) analysis. By using MCS, it is possible to track the failure modes for each generated sample. Despite being computationally intensive, MCS is considered a robust method due to the requirement of a significant number of sample points, particularly when using crude sampling techniques. Nonetheless, this approach is favored as a benchmark tool when precision is valued more than computational efficiency.

A reliability assessment comprises two primary components: stochastic variables and limit-state functions. Stochastic variables, which are gathered in vector x, represent the uncertainties in the problem. The limit-state function, denoted as g, defines the occurrence for which the probability is being determined. For instance, in the fundamental reliability scenario, the main objective is to calculate the probability of system failure, also known as exceedance probability (EP). Failure takes place when the system's capacity, $R(x)$, surpasses the demand, $S(x)$, resulting in the limit-state function, as shown in Eq. 15.

$$g(x) = R(x) - S(x) \tag{15}$$

The exceedance probability, which is shown by G, is related to the reliability index denoted by β based on Eq. 16.

$$G = \Phi(-\beta) \tag{16}$$

where Φ is the univariate standard normal cumulative distribution function (CDF).

Finally, the exceedance probability in the sampling method is calculated using a step function, $I(x)$, by Eq. 17.

$$G = \int_{-\infty}^{+\infty} \dots \int_{-\infty}^{+\infty} I(x) f_x(x) dx \tag{17}$$

where $f_x(x)$ is the joint probability density function of random variables x, and the number of integrals equals the number of variables in x, denoted here by n. Also, $I(x)$ is defined as Eq. 18.

$$I(x) = \begin{cases} 1, & g(x) \le 0 \\ 0, & g(x) > 0 \end{cases} \tag{18}$$

Reliability analysis are carried out to assess the structural performance in real-world conditions characterized by uncertainties in loadings and structural material and details. While a basic structural analysis can determine whether a structure will fail in specific conditions, in situations where the structural demand or resistance is uncertain, a reliability assessment is employed to assess the probability of failure. The sampling-based reliability assessment is carried out to investigate the vulnerability of a steel building with an SPSW system designed for seismic forces when exposed to blast explosive loading. In this study, the limit-state function has been chosen for checking the maximum drift ratio with 1.5%. In order to perform the stochastic nonlinear finite element analysis, the Rtx software has been linked to OpenSees software [49]. An overall view of the procedure has been presented in Fig. 11.

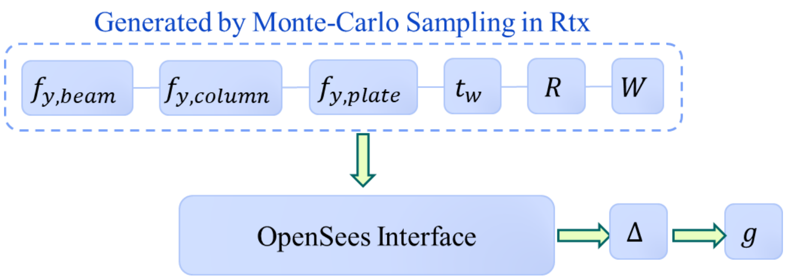

Fig. 11. Overall view of stochastic finite element analysis.

In this study, the maximum inter-story drift ratio was selected as the engineering demand parameter for defining structural performance under blast loading. The failure limit state was defined as exceedance of a 1.5% inter-story drift ratio. This value was selected based on the allowable story drift limits specified in ASCE 7 for building structures and was adopted as a practical performance-based deformation threshold. Although blast loading is different from seismic loading in terms of duration and loading mechanism, the ASCE 7 drift limit provides a recognized engineering basis for defining excessive lateral deformation.

In addition, because the present study is a probabilistic and comparative reliability assessment, a consistent drift threshold is required to classify the structural response of all Monte Carlo simulations into safe and failed cases. Therefore, the 1.5% drift ratio was used as a uniform limit state to evaluate and compare the vulnerability of the SPSW structure under different blast-loading scenarios and uncertainty realizations (Eq. 19). Exceedance of this threshold was interpreted as reaching an unacceptable deformation/damage state, not necessarily global collapse of the structure.

$$g(x) = 0.015 - \Delta(x) \tag{19}$$

Uncertainty in material properties, geometric characteristics and blast parameters is unavoidable. Even with the advancements in manufacturing technologies and precision measuring devices, the precise values of these parameters remain challenging to ascertain. As a result, tolerance ranges for the parameters have been employed instead. Every parameter is allocated a fixed value and a distribution derived from pertinent literature or building standards, and the reliability assessment is carried out in the manner outlined in the preceding section. Table 4 provides the variables, related distributions, and values employed for the fixed analysis.

Table 4. Variable, distribution, and mean values [50].

Uncertainties			
Variable	**Distribution**	**Mean**	**CoV**
t_w	Lognormal	1 mm	0.03
$f_{y,\ plate}$	Lognormal	1.38 × 2400 kg/cm^2	0.07
$f_{y,\ column}$	Lognormal	1.38 × 2400 kg/cm^2	0.07
$f_{y,\ beam}$	Lognormal	1.495 × 2400 kg/cm^2	0.07
R	Lognormal	20 m	0.03
W	Normal	1814 kg	0.001

7. Results and discussions

Fig. 12 illustrates the convergence behavior of the Monte Carlo simulation results as the number of generated samples increases. In this analysis, each Monte Carlo sample represents a realization of the uncertain parameters listed in Table 4. For each sample, a nonlinear dynamic analysis was performed, and the maximum inter-story drift ratio was obtained. If the calculated drift ratio exceeded the selected performance limit of 1.5%, the sample was classified as failure. The cumulative failure probability was then calculated as the ratio of failed samples to the total number of generated samples. By progressively increasing the number of samples, the convergence of the estimated failure probability was evaluated, which resulted in the curve shown in Fig. 12.

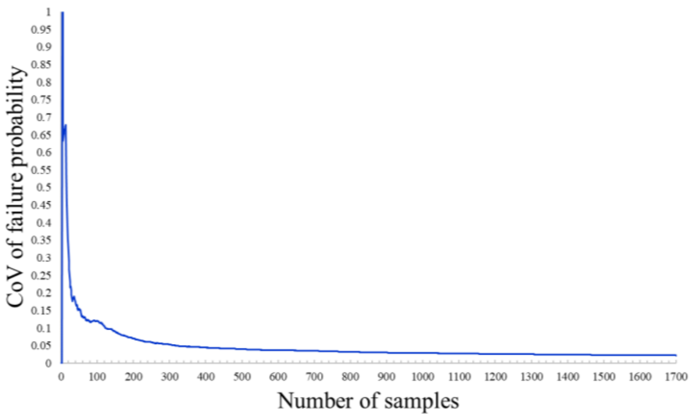

(a)

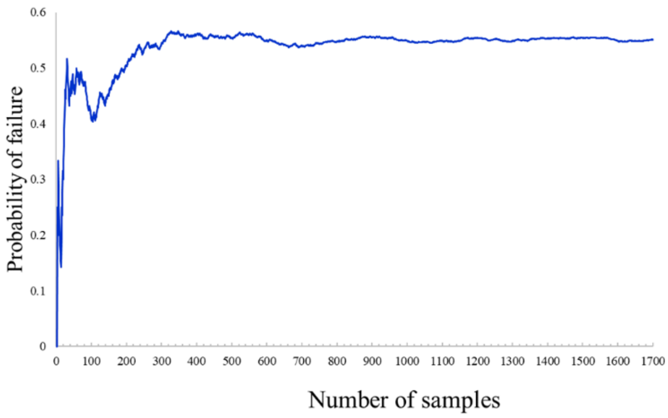

(b)

Fig. 12. (a) CoV for probability of failure; and (b) probability of failure.

The stability of the Monte Carlo estimator was verified by examining the convergence of the failure probability as the number of samples approached 1700. The observed stabilization of the estimator, characterized by a Coefficient of Variation of approximately 0.02, confirms that the adopted sample size is sufficient to provide a stable estimate for the investigated performance limit state. In addition, the probabilistic characteristics of the random variables used in the Monte Carlo simulation are summarized in Table 4. As shown in this table, the uncertainties considered in the reliability analysis include the web plate thickness, yield stress of the web plate, yield stress of columns and beams, standoff distance, and charge weight. The corresponding mean values and coefficients of variation are reported in Table 4. This information clarifies the probabilistic input parameters used for generating the Monte Carlo samples and improves the reproducibility of the reliability analysis.

1700 samples were generated using Monte Carlo sampling method. Considering the uncertainties in material properties of steel for columns, beams, and web plate, web plate thickness, standoff distance, and charge weight, the fragility curve can be obtained as shown in Fig. 13. As is evident in Fig. 13, the probability that the maximum drift ratio surpasses the 1.5% limit is 55%, and the reliability index is equal to -0.129. This shows that a typical steel structure with an SPSW system designed for a high seismic area is highly vulnerable when exposed to an explosive blast induced by a truck vehicle. However, in order to avoid non-economical design sections, it is possible to decrease the hazard by defining safety circles to stop suspicious vehicles from entering the residential areas. Fig. 12a shows that after generation of 1700 samples, the failure probability has converged to an almost constant value with a Coefficient of Variation (CoV) equal to 0.02.

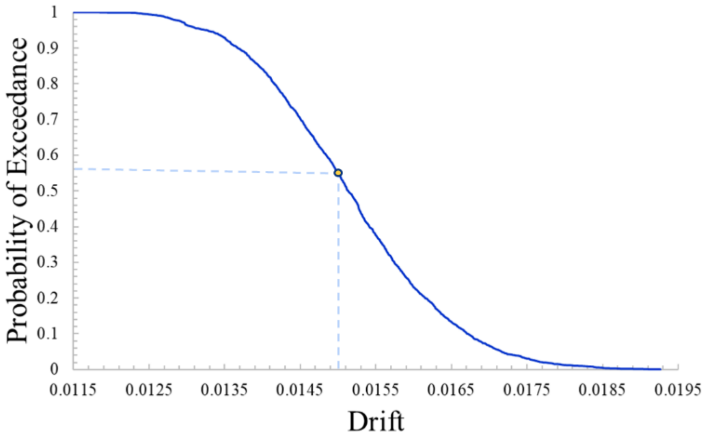

Fig. 13. Structural reliability under explosive blast considering the defined variable.

From an engineering performance perspective, the selected 1.5% inter-story drift ratio represents a deformation-based limit state for evaluating the serviceability and damage level of the SPSW system under extreme blast loading. Exceedance of this threshold does not necessarily indicate global collapse of the structure; rather, it implies that the structure has reached an unacceptable level of lateral deformation for the adopted performance criterion. Therefore, the calculated failure probability of 55% and the corresponding reliability index of β = -0.129 indicate a high likelihood of exceeding the selected drift-based performance limit under the considered truck-borne blast scenario. This result suggests that, although the SPSW building was designed for a high seismic region, its deformation demand under extreme blast loading can exceed the acceptable performance range, emphasizing the need for appropriate protective measures such as controlling the minimum standoff distance.

Also, a sensitivity analysis was performed. As depicted in Fig. 14, the results showed that the reliability index is mostly affected by the web plate thickness. To identify the relative importance of the uncertain input parameters, a sensitivity analysis was performed using the Monte Carlo simulation results. In this study, the sensitivity index was expressed as $dP_f/dStdv$, where P_f is the probability of failure, and $Stdv$ denotes the standard deviation of each random variable. This index represents the rate of change in the estimated failure probability with respect to the standard deviation of a given uncertain parameter. Therefore, a larger absolute value of $dP_f/dStdv$ indicates that the probability of failure is more sensitive to the uncertainty associated with that parameter.

The parameter influence was evaluated by perturbing the standard deviation of each random variable individually while keeping the mean values and the statistical properties of the other variables unchanged. For each perturbation, the Monte Carlo simulations were repeated, and the corresponding change in failure probability was calculated. The sensitivity index was then obtained as the ratio between the change in probability of failure and the change in the standard deviation of the considered parameter.

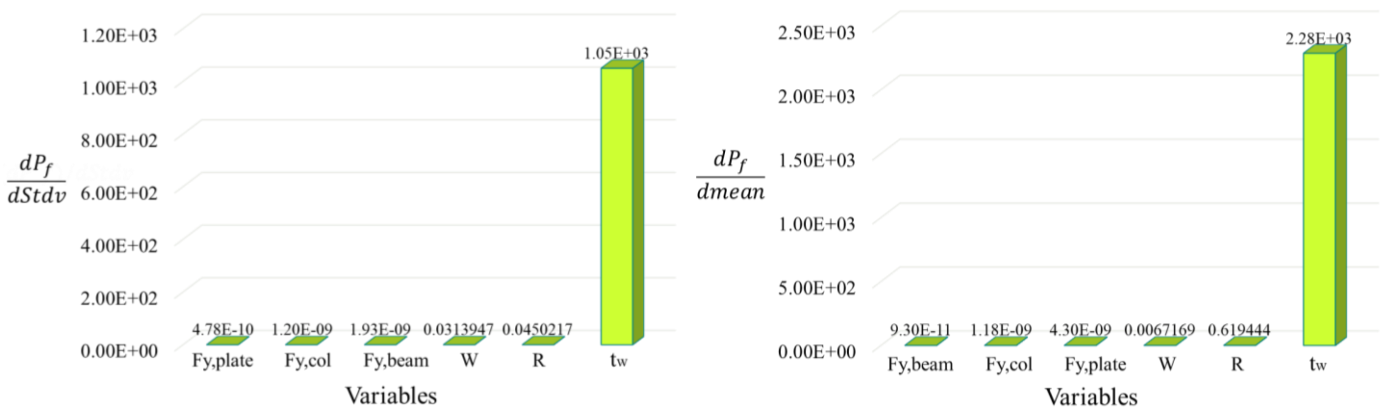

(a) **(b)**

Fig. 14. Sensitivity analysis based on: (a) $\frac{dP_f}{dStdv}$; and (b) $\frac{dP_f}{dmean}$.

8. Conclusions

This paper performs a reliability analysis on a steel structure with a steel plate shear wall system that is basically designed for gravitational and seismic forces in a high seismic area based on the ASCE7-16 after being subjected to blast loading. The stochastic nonlinear dynamic finite element analysis has been carried out considering the inherent uncertainties in the variables such as web plate thickness of SPSW, yield stress of steel, standoff distance, and charge weight. A finite element model has been built and verified using the so-called strip model to capture the behavior of the steel structure after being subjected to explosive blast. 1700 analysis were done using samples that were generated based on the Monte Carlo sampling method with Rtx software. The following conclusions can be drawn:

- By considering W, R, web plate thickness, web plate yield stress, beam and column yield stress as random variables, the failure probability of a steel frame subjected to blast loading induced by a delivery truck is 55 percent. Also, the corresponding reliability index is equal to -0.129.
- Using sampling-based sensitivity analysis, web plate thickness, standoff distance, and explosion charge weight turn out to be the most important parameters in the failure probability of a steel frame.
- By performing histogram sampling, the exceedance probability curve of the drift ratio is obtained.
- Monte Carlo sampling can be used as an appropriate method to investigate the reliability level of steel structures with SPSW system.
- Rtx software can be used as an engineer-friendly reliability assessment tool to evaluate the reliability level of the designed structures exposed to blast loadings.

Statements & declarations

Author contributions

Zeinab Meghdadi: Investigation, Methodology, Resources, Writing - Original Draft, Writing – Review & Editing.

Mohammad Shabanlou: Investigation, Methodology, Resources, Writing - Original Draft, Writing – Review & Editing.

Funding

The authors received no financial support for the research, authorship, and/or publication of this article.

Data availability

The data presented in this study will be available on interested request from the corresponding author.

Declarations

The authors declare no conflict of interest.

References

[1] Shabanlou, M., Moghaddam, H., Saedi Daryan, A. The Effect of Geometry on Structural Behavior of Buildings with Steel Plate Shear Wall System Subjected to Blast Loading. International Journal of Steel Structures, 2021; 21: 650–665. doi:10.1007/s13296-021-00463-4.

[2] Sarcheshmehpour, M., Shabanlou, M., Meghdadi, Z., Estekanchi, H. E., Mofid, M. Seismic evaluation of steel plate shear wall systems considering soil-structure interaction. Soil Dynamics and Earthquake Engineering, 2021; 145: 106738. doi:10.1016/j.soildyn.2021.106738.

[3] Alvanchi, A., Jafari, M. A., Shabanlou, M., Meghdadi, Z. A novel public-private-people partnership framework in regeneration of old urban neighborhoods in Iran. Land Use Policy, 2021; 109: 105728. doi:10.1016/j.landusepol.2021.105728.

[4] Stewart, M. G., Netherton, M. D., Rosowsky, D. V. Terrorism Risks and Blast Damage to Built Infrastructure. Natural Hazards Review, 2006; 7: 114–122. doi:10.1061/(ASCE)1527-6988(2006)7:3(114).

[5] Al-Hababheh, O., Stewart, M. Structural Reliability Analysis of Unreinforced Brick Masonry Walls Subject to Explosive Blast Loading. In: Proceedings of the First International Conference of Protective Structures (ICPS); 2010 Sep–Oct; Manchester, United Kingdom.

[6] Shi, Y., Stewart, M. G. Spatial reliability analysis of explosive blast load damage to reinforced concrete columns. Structural Safety, 2015; 53: 13–25. doi:10.1016/j.strusafe.2014.07.003.

[7] Stewart, M. G., Netherton, M. D. Reliability-Based Design Load Factors for Explosive Blast Loading. Journal of Performance of Constructed Facilities, 2015; 29: 1–8. doi:10.1061/(ASCE)CF.1943-5509.0000709.

[8] Netherton, M. D., Stewart, M. G. Blast Load Variability and Accuracy of Blast Load Prediction Models. International Journal of Protective Structures, 2010; 1: 543–570. doi:10.1260/2041-4196.1.4.543.

[9] Stochino, F. RC beams under blast load: Reliability and sensitivity analysis. Engineering Failure Analysis, 2016; 66: 544–565. doi:10.1016/j.engfailanal.2016.05.003.

[10] Shabanlou, M., Mofid, M., Eslami, M., Kodur, V., Meghdadi, Z., Tavakoli, A. Experimental, analytical and numerical investigation on the effects of different shear reinforcement on residual post-fire behavior of reinforced concrete deep beams. Structure and Infrastructure Engineering, 2025; 1–18. doi:10.1080/15732479.2025.2456466.

[11] Thomas, R. J., Steel, K., Sorensen, A. D. Reliability analysis of circular reinforced concrete columns subject to sequential vehicular impact and blast loading. Engineering Structures, 2018; 168: 838–851. doi:10.1016/j.engstruct.2018.04.099.

[12] Astaneh-Asl, A., Zhao, Q. Cyclic tests of steel shear walls. Research project. Berkeley: Department of Civil and Environmental Engineering, University of California, 2001.

[13] Astaneh-Asl, A. Seismic Behavior and Design of Composite Steel Plate Shear Walls. Berkeley (CA): Steel Technical Information & Product Service (Steel TIPS); 2002. Report No.: 01.

[14] Astaneh-Asl, A. Steel Plate Shear Walls. In: U.S.-Japan Workshop on Seismic Fracture Issues in Steel Structures; 2000 Feb; San Francisco, California. p. 1–12.

[15] Berman, J. W., Bruneau, M. Capacity Design of Vertical Boundary Elements in Steel Plate Shear Walls. Engineering Journal, 2008; 45: 57–72. doi:10.62913/engj.v45i1.925.

[16] Elgaaly, M., Caccese, V., Du, C. C. Postbuckling Behavior of Steel-Plate Shear Walls under Cyclic Loads. Journal of Structural Engineering-asce, 1993; 119: 588–605. doi:10.1061/(ASCE)0733-9445(1993)119:2(588).

[17] Bahrebar, M., Lim, J. B. P., Clifton, G. C., Zirakian, T., Shahmohammadi, A., Hajsadeghi, M. Perforated steel plate shear walls with curved corrugated webs under cyclic loading. Structures, 2020; 24: 600–609. doi:10.1016/j.istruc.2020.01.047.

[18] Zirakian, T., Zhang, J. Seismic design and behavior of low yield point steel plate shear walls. International Journal of Steel Structures, 2015; 15: 135–151. doi:10.1007/s13296-015-3010-8.

[19] Emami, F., Mofid, M. On the hysteretic behavior of trapezoidally corrugated steel shear walls. The Structural Design of Tall and Special Buildings, 2014; 23: 94–104. doi:10.1002/tal.1025.

[20] Choi, I.-R., Park, H.-G. Steel Plate Shear Walls with Various Infill Plate Designs. Journal of Structural Engineering, 2009; 135: 785–796. doi:10.1061/(ASCE)0733-9445(2009)135:7(785).

[21] Meghdadi, Z., Khaloo, A. Experimental, theoretical and numerical study on flexural behavior of hybrid steel-GFRP reinforced concrete slabs. Structural Concrete, 2025; 26: 739–758. doi:10.1002/suco.202301085.

[22] Meghdadi, Z., Khaloo, A., Ashour, A. Residual structural performance of fire-exposed concrete slabs reinforced with hybrid GFRP-steel bars: Experimental and numerical studies. Structures, 2025; 80: 109757. doi:10.1016/j.istruc.2025.109757.

[23] Shabanlou, M., Meghdadi, Z., Ghaffar, S. H. Experimental and analytical study of the residual performance of reinforced concrete deep beams with circular web openings. Results in Engineering, 2025; 25: 104229. doi:10.1016/j.rineng.2025.104229.

[24] Shabanlou, M., Mofid, M., Tavakoli, A. Post-fire performance of GFRP reinforced concrete deep beams: experimental and numerical study. Structure and Infrastructure Engineering, 2024; 22: 1280–1298. doi:10.1080/15732479.2024.2382131.

[25] Shabanlou, M., Mofid, M., Tavakoli, A. Experimental and Numerical Study on the Behavior of Reinforced Concrete Deep Beams with Normal-Strength and High-Strength Concrete After Being Exposed to Fire. Arabian Journal for Science and Engineering, 2024; 49: 13457–13476. doi:10.1007/s13369-023-08676-x.

[26] Alinia, M. M. A study into optimization of stiffeners in plates subjected to shear loading. Thin-Walled Structures, 2005; 43: 845–860. doi:10.1016/j.tws.2004.10.008.

[27] American Institute of Steel Construction (AISC). ANSI/AISC 360-16: Specification for Structural Steel Buildings. Farmington Hills (MI): AISC; 2016.

[28] American Institute of Steel Construction (AISC). AISC 341-16: Seismic Provisions for Structural Steel Buildings. Farmington Hills (MI): AISC; 2016.

[29] American Society of Civil Engineers (ASCE). ASCE 7-10: Minimum Design Loads for Buildings and Other Structures. Reston (VA): ASCE; 2010.

[30] Sabelli, R., Bruneau, M. Steel Design Guide 20: Steel Plate Shear Wall. First ed. Farmington Hills (MI): AISC; 2007.

[31] Mazzoni, S., McKenna, F., H. Scott, M., L. Fenves, G. OpenSees Command Language Manual. Oakland (CA): University of California; 2006.

[32] Thorburn, L. J., Kulak, G. L., Montgomery, C. J. Analysis of Steel Plate Shear Walls. Calgary (CA): University of Alberta; 1983. Report No.: 107.

[33] Jalali, S. A., Banazadeh, M. Computer-based evaluation of design methods used for a steel plate shear wall system: Computer-Based Evaluation of SPSW Design Methods. The Structural Design of Tall and Special Buildings, 2016; 25: doi:10.1002/tal.1290.

[34] Jalali, S. A., Banazadeh, M. Development of a new deteriorating hysteresis model for seismic collapse assessment of thin steel plate shear walls. Thin-Walled Structures, 2016; 106: 244–257. doi:10.1016/j.tws.2016.05.008.

[35] Jalali, S. A., Darvishan, E. Seismic demand assessment of self-centering steel plate shear walls. Journal of Constructional Steel Research, 2019; 162: 105738. doi:10.1016/j.jcsr.2019.105738.

[36] Sabouri-Ghomi, S., Sajjadi, S. R. A. Experimental and theoretical studies of steel shear walls with and without stiffeners. Journal of Constructional Steel Research, 2012; 75: 152–159. doi:10.1016/j.jcsr.2012.03.018.

[37] Federal Emergency Management Agency (FEMA). FEMA 427: Risk Management Series FEMA 427 Primer for design of commercial buildings to mitigate terrorist attacks. Washington, D.C. (US): ASCE; 2003.

[38] Ngo, T., Mendis, P., Gupta, A., Ramsay, J. Blast Loading and Blast Effects on Structures – An Overview. Electronic Journal of Structural Engineering, 2007; 7: 76–91. doi:10.56748/ejse.671.

[39] Moghimi, H., Driver, R. G. Performance assessment of steel plate shear walls under accidental blast loads. Journal of Constructional Steel Research, 2015; 106: 44–56. doi:10.1016/j.jcsr.2014.11.010.

[40] Needham, C. E. Blast Waves (Shock Wave and High Pressure Phenomena). First ed. Berlin (DE): Springer, Heidelberg; 2010. doi:10.1007/978-3-642-05288-0.

[41] Iranian National Building Code, Part 21. 2nd ed. Tehran (IR): Building and Housing Research Center (BHRC); 2016.

[42] U.S. Department of Defence. UFC 3-340-02: Unified Facilities Criteria (UFC) Structures to Resist the Effects of Accidental Explosions. Arlington County (VA): UFC; 2008.

[43] Dusenberry, D. O. Handbook for Blast Resistant Design of Buildings. First ed. Hoboken (NJ): John Wiley & Sons, Inc; 2010. doi:10.1002/9780470549070.

[44] U.S. Department of Homeland Security. DHS Bomb Threat Stand-Off Chart. 2010. https://publicintelligence.net/dhs-bomb-threat-stand-off-chart/. (Accessed February 2010).

[45] Moghaddam, H., Shabanlou, M., Saedi Daryan, A. Study of the Blast Resistance of Seismically Designed Steel Plate Shear Wall Frames. Sharif Journal of Civil Engineering, 36.2: 117–129. doi:10.24200/j30.2019.53613.2562.

[46] Brode, H. L. Numerical Solutions of Spherical Blast Waves. Journal of Applied Physics, 1955; 26: 766–775. doi:10.1063/1.1722085.

[47] Newmark, N. M., Hansen, R. J. Design of blast-resistant structures. First ed. Columbus (OH): McGraw-Hill; 1961.

[48] Shoaei, P., Mahsuli, M. Reliability-based design of steel moment frame structures isolated by lead-rubber bearing systems. Structures, 2019; 20: 765–778. doi:10.1016/j.istruc.2019.06.020.

[49] Talebiyan, H., Mahsuli, M. Sampling-Based Reliability Sensitivity Analysis Using Direct Differentiation. ASCE-ASME Journal of Risk and Uncertainty in Engineering Systems, Part A: Civil Engineering, 2020; 6: 04020015. doi:10.1061/AJRUA6.0001050.

[50] Jordaan, I. Decisions under uncertainty: probabilistic analysis for engineering decisions. First ed. Cambridge (UK): Cambridge University Press; 2005.